sustainability

MDPI

Article

Developmental Characteristics and Genesis of Ground Fissures in Wangjiacun, Emei Plateau, Yuncheng Basin, China

Feida Li [1], Feiyong Wang [1,2,3,4,*], Fujiang Wang [1] and Guoqing Li [1]

[1] Institute of Geosafety, School of Engineering and Technology, China University of Geosciences Beijing, Beijing 100083, China; fd-li@email.cugb.edu.cn (F.L.); fujiang.wang@email.cugb.edu.cn (F.W.); guoqing.li@email.cugb.edu.cn (G.L.)
[2] Key Laboratory of Earth Fissures Geological Disaster, Ministry of Natural Resources (Geological Survey of Jiangsu Province), Nanjing 210018, China
[3] Observation and Research Station of Ground Fissure and Land Subsidence, Ministry of Natural Resources, Xi'an 710054, China
[4] Engineering and Technology Innovation Center for Risk Prevention and Control of Major Project Geosafety, MNR, Beijing 100083, China
* Correspondence: fy-wang@cugb.edu.cn

Abstract: The Yuncheng Basin is part of the Fenwei Graben System, which has developed ground fissure hazards that have caused serious damage to farmland, houses, and roads and have brought about huge economic losses. Located in Wanrong County on the Emei Plateau in the northwestern part of the Yuncheng Basin in China, the Wangjiacun ground fissure is a typical and special ground fissure developed in loess areas, and its formation is closely related to tectonic joints and the collapsibility of loess. In order to reveal the formation and genesis of the Wangjiacun ground fissure, the geological background, developmental characteristics, and genesis pattern of the Wangjiacun ground fissures were studied in detail. A total of three ground fissures have developed in this area: a linear fissure (f1) is distributed in an NNE-SSW direction, with a total length of 334 m; a circular fissure (f2) is located near the pool, with a total length of 720 m; f2-1, a linear fissure near f2, has a fissure length of 110 m and an NE orientation. This study shows that tectonic joints in loess areas are the main controlling factors of the linear fissure (f1); differential subsidence in the pool caused by collapsible loess is the main source of motivation for the formation of the circular fissures (f2, f2-1), and tensile stresses produced by the edges of subsidence funnels lead to the cracking of shallow rock and soil bodies to form ground fissures (f2, f2-1). This study enriches the theory of ground fissure genesis and is of great significance for disaster prevention and the mitigation of ground fissures in loess areas.

Keywords: ground fissures; Emei Plateau; Yuncheng Basin; tectonic action; collapsible loess

check for updates

Citation: Li, F.; Wang, F.; Wang, F.; Li, G. Developmental Characteristics and Genesis of Ground Fissures in Wangjiacun, Emei Plateau, Yuncheng Basin, China. *Sustainability* **2024**, *16*, 3649. https://doi.org/10.3390/su16093649

Academic Editor: Antonio Miguel Martínez-Graña

Received: 17 March 2024
Revised: 13 April 2024
Accepted: 24 April 2024
Published: 26 April 2024

Copyright: © 2024 by the authors. Licensee MDPI, Basel, Switzerland. This article is an open access article distributed under the terms and conditions of the Creative Commons Attribution (CC BY) license (https://creativecommons.org/licenses/by/4.0/).

1. Introduction

Ground fissures are geological hazards that produce linear fractures in shallow bodies of rock and soil, triggered by internal and external dynamic geology and by human activities [1–4]. Ground fissures can be classified as tectonic and non-tectonic depending on the cause. Ground fissures are widely distributed in China and abroad, mainly in the Fenwei Basin in Northwest China and in North America and Africa [5–8]. In addition, ground fissures are continuously destructive and difficult to avoid, so their existence can lead to cracks in agricultural land, houses, roads, and other buildings, posing a serious geosafety risk and causing incalculable damage to states [9,10]. Ground fissures are mostly developed in the interior of basins and are closely related to tectonic action and human activities [5]. The Wangjiacun ground fissure is located above the Emei Plateau in the Yuncheng Basin, belonging to a typical and special collapsible loess-type ground fissure, which is related to tectonic joints and collapsible loess.

As a global geohazard, this particular geological hazard has received attention from scholars at home and abroad, with basin-type ground fissures (those developed in basins and valleys) being one of the main focuses of research. Some scholars believe that faults or pumping a certain factor affects the formation of ground fissures in basins. Underneath some ground fissures, hidden faults can be detected, and fissures may be extensions of these faults at the surface [11]. When earthquakes occur, they cause tensile stresses to build up in the ground, creating ground fissures [12]. The massive extraction of groundwater, resulting in the compression of aquifers and uneven settlement, results in the tensile cracking of the ground surface to form ground fissures [6,13]. In addition, there are also scholars who believe that ground fissures are not formed by the influence of a single factor but are the result of the joint action of faults and pumping water [1,14–18]. In the absence of the formation of bedrock faults, seismic elastic strains originating at depth propagate upward through the sediments and, in combination with heavy rainfall, produce ground fissures at the surface [1]. The Fenwei Basin in China has become a typical area of basin ground fissures for domestic ground fissure research due to its special and representative regional location [5]. Studies on the Fenwei Basin have focused on the sub-basins of the Fenwei Basin including the Datong Basin, Taiyuan Basin, Linfen Basin, Yuncheng Basin, and Weihe Basin. The tectonic activity in these basins is intense, and it controls the occurrence and intensity of ground fissures and is also a fundamental factor in the formation of ground fissures [4,19,20]. Moreover, the excessive extraction of groundwater can also affect the ground fissures in these basins, promoting their development. For example, it can cause pre-existing concealed faults [15,21,22] to become active, cause frontal faults to continue growing and expose them at the surface [23], or cause existing ground fissures to increase in size [24].

The Yuncheng Basin is one of the most widely distributed areas of basin ground fissures in Shanxi Province. According to geomorphological divisions, research on destructive ground fissures in the basin mainly focuses on the graben of the Qinglong River Valley, with a small number distributed on the Emei Plateau. The ground fissures in the Qinglong graben are connected to faults, and the formation process of ground fissures in the Qinglong graben can be divided into three stages: firstly, the regional tensile tension in the basin prompted the active fractures to extend and creep and slip, and formed a tectonic rupture base within the shallow surface geotechnical body; subsequently, the pumping effect of excessive groundwater caused the internal rupture of the geotechnical body to expand to the surface, and finally, surface water erosion induced the rupture of the geotechnical and the outcrop of the ground fissure was eventually formed [25]. The Emei Plateau in the northern part of the Yuncheng Basin developed a large area of loess plateau, and the tectonic joints and collapsible characteristics of loess are closely related to the formation of ground fissures. Scholars have found that loess is more susceptible to fissuring under tensile stress. And the main reason for the development of ground fissure hazards in loess areas is the weak tensile strength, loose structure, and highly collapsible loess [26]. Typical examples include the Xuedian ground fissure, a 140 m long and 1 m wide ground fissure that appeared after a rainstorm [27].

The means of research on ground fissures have been enriched in recent years and are not only limited to traditional research methods, but also include model studies and numerical modeling. Academics modeling the geological and hydrogeological settings of the pumping-caused ground fissures [28] undertook a series of physical simulation tests on a large-scale soil sample [29] and simulated the seismic response of an active ground fissure site [30]. Through model studies and numerical modeling, scholars have further deepened their research on ground fissures.

There are relatively few studies on collapsible loess ground fissures, and the Wangjia-cun ground fissure in the Yuncheng Basin is both typical and special, which is formed by the joint action of loess tectonic joints and collapsible loess. The study of its development characteristics and mechanisms can enrich the theory of ground fissure genesis, which is of great significance for disaster prevention and mitigation.

The paper is structured as follows: Section 2 presents the geological background of the study area; Section 3 presents the developmental characteristic of the ground fissures; Section 4 presents the discussion; Section 5 presents conclusion.

2. Geological Background

The Fenwei Basin is special and representative of the regional tectonic setting. The Fenwei Basin is located between the Ordos Block and the North China Block, with a general NNE orientation and an "S"-type spread in plan [5]. The Yuncheng Basin is located in the southern part of the Fenwei graben system (Figure 1), between the Shanxi fault zone and the Weihe fault zone. The Yuncheng Basin is a mature basin with an NE orientation, dominated by vertical fault-slip movements.

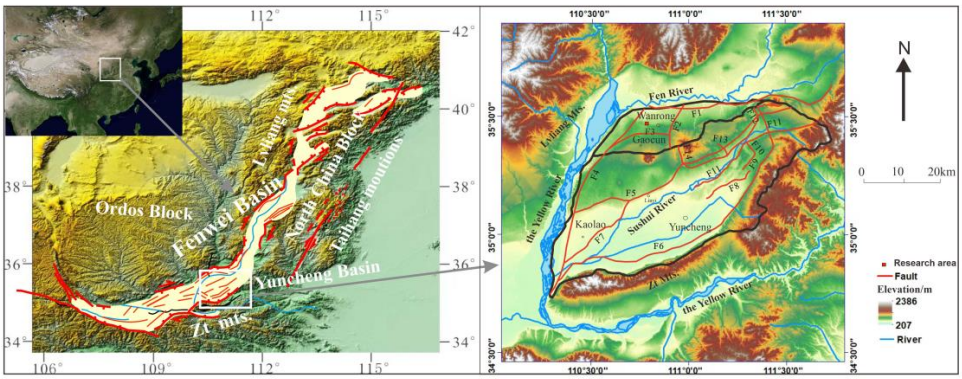

Figure 1. Regional tectonics and rupture of the Yuncheng Basin; F1—northern edge of the Emei Plateau Fault, F2—Xishe-Zaidian Fault, F3—Wusu-Jiacun Fault, F4—eastern part of the Yellow River Valley Fault, F5—southern edge of the Emei Plateau Fault, F6—Zhongtiao Mountain Fault, F7—Caomu Plateau Fault, F8—eastern edge of Mingjiao Heights Fault, F9—Wenxi Daze-Xiaoze Fault, F10—Shaqu River Fault, F11—western edge of Mingjiao Heights Fault, F12—Wendian-Weijia Fault, F13—Shenbai-Longdao Fault, F14—Sanluli-Hanxue Fault.

The Yuncheng Basin can be divided into four major tectonic geomorphic units from north to south: the Emei Plateau uplift zone, the Yuncheng fault depression basin area, the Zhongtiao Mountain fault block uplift area, and the Yellow River Valley trench zone on the western side (Figure 2). The boundaries between these structural units are marked by faults, such as the eastern part of the Yellow River Valley Fault (F4), the southern edge of the Emei Plateau Fault (F5), and the Zhongtiao Mountain Fault (F6). The study area is located on the northern side of the Emei Plateau in the Yuncheng Basin, surrounded by faults. To the north of the study area is the northern edge of the Emei Plateau Fault (F1); the length of the fault is 85 km, the tendency is north-west oriented, the fault distance is 200~1000 m, and the nature of the fault is a shovel-type positive fault. On the east side of the study area is the Xishe-Zaidian Fault (F2), which is a concealed fault with a length of 25 km, a tendency toward a south-east-east direction, and a positive fault. The fault on the south side of the study area is the Wusu-Jiacun Fault (F3), which is the dividing line between the Emei Class I and Class II plateaus, with a nearly east–west strike and a length of about 25 km. On the west side of the study area is the eastern section of the eastern part of the Yellow River Valley Fault (F4), with a length of 70 km, a tendency toward a north-west-west direction, and a positive fault.

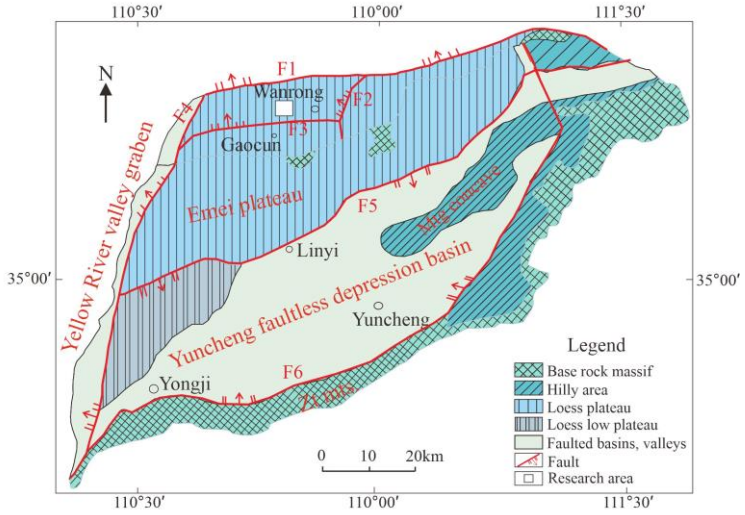

Figure 2. Geomorphology of the Yuncheng Basin and distribution of major faults; F1—northern edge of the Emei Plateau Fault, F2—Xishe-Zaidian Fault, F3—Wusu-Jiacun Fault, F4—eastern part of the Yellow River Valley Fault, F5—southern edge of the Emei Plateau Fault, F6—Zhongtiao Mountain Fault.

The study area is located in the northern part of the Yuncheng Basin, on the Emei Plateau, which is predominantly covered by quaternary loess (Figure 3). The loess itself exhibits weak tensile strength and is characterized by its collapsibility. According to their formation ages, the quaternary loess deposits can be divided into two layers: the Malan loess of the Late Pleistocene (Q3) and the Lishi loess of the Middle Pleistocene (Q2) (Figure 3). The Yuncheng Basin is surrounded by mountains on three sides, with only one river, the Xushui River, flowing through it. To the north of the basin lies the Fen River, separated from the Xushui River by the Emei Plateau. The groundwater aquifer is strictly controlled by geological structures and landform features, leading to significant environmental differences among different areas (Figure 4). Therefore, there are considerable variations in the structure of aquifers both horizontally and vertically. Groundwater recharge mainly comes from atmospheric precipitation and underground runoff. The Yuncheng Basin experiences a temperate continental monsoon climate with four distinct seasons and annual rainfall of 500 mm.

System	Series	Symbol	Histogram	Th/m	Type	Description
Quaternary	Upper Pleistocene	Q3		8.2	Malan Loess Paleosol	Light yellow, loose, macroporous with vertical joints,with a layer of paleosol
	Middle Pleistocene	Q2		86.3	Lishi Loess Paleosol	Grayish brown,loose, no bedding, sandwiched with multi-layer reddish brown paleosol

Figure 3. Quaternary stratigraphic histogram of the Emei Plateau.

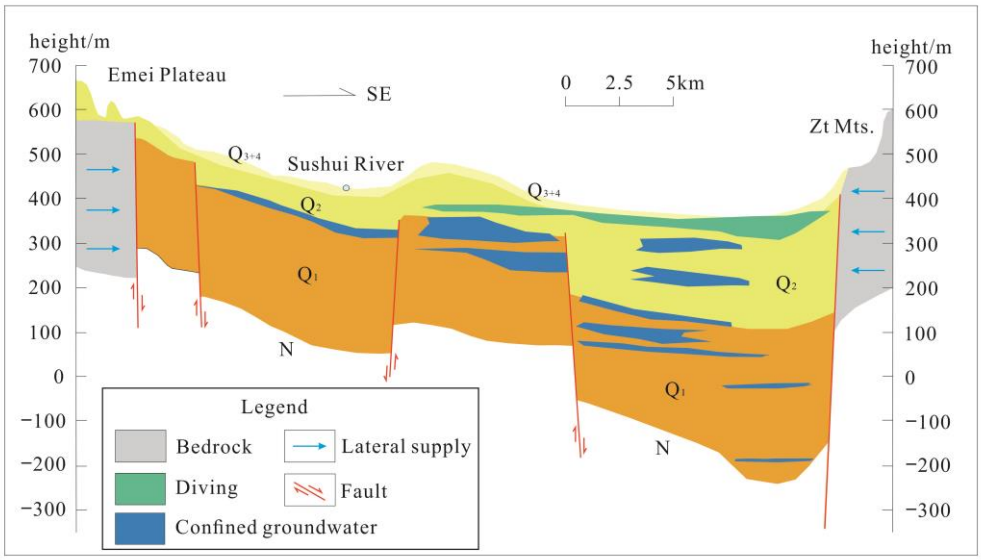

Figure 4. Lithology and hydrography of the Yuncheng Basin.

3. Developmental Characteristics

3.1. Plane Distribution

One of the Wangjiacun ground fissures, f1, is linearly distributed, with a fissure length of 335 m and good continuity through the whole village. The overall orientation of the ground fissure is nearly NNE-SSW, with the fissure appearing from the north of the village until it approaches the south of the village, where the fissure changes from a nearly NS orientation to an NE orientation. In addition, there is an annular fissure, f2, in the Wangjiazhuang ground fissure with a length of 720 m. The fissure is nearly elliptical in shape. The fissure is located in an orchard to the west of the village, and the middle part of the fissure is a pool. A linear fissure, f2-1, exists at the edge of the pool, which is 110 m long and has an NE orientation (Figure 5).

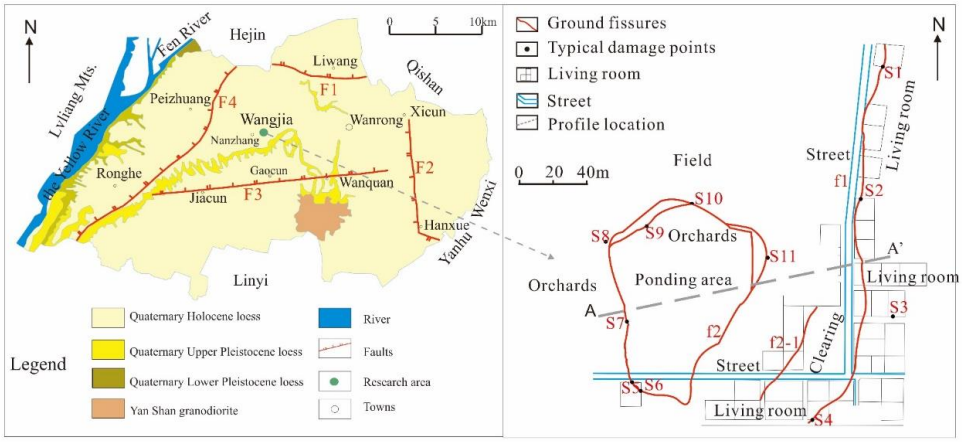

Figure 5. Ground fissure plan view of Wangjiacun; F1—northern edge of the Emei Plateau Fault, F2—Xishe-Zaidian Fault, F3—Wusu-Jiacun Fault, F4—eastern part of the Yellow River Valley Fault.

3.2. Profile Structure

After investigation, it was found that the ground fissure profiles in the loess region have a similar profile structure. Combined with field research and the existing literature [31–33], it is not difficult to find that ground fissures developed in loess bodies tend to open up to a greater extent near the surface, while at a deeper location below the surface, the ground fissures are relatively small in width and tend to be in a closed state. This phenomenon occurs because as the burial depth increases, the confining pressure exerted on the surrounding soil gradually increases. For soils below the surface, the rupture mode changes gradually as the burial depth increases, transforming from a shallow tensile rupture to a deep shear rupture. This transition generally occurs at around 10 m below the surface, with tensile failure predominating above 10 m and shear failure predominating below 10 m. Additionally, the observed ground fissures in the soil often exhibit steep angles. The profile structure of the ground fissures in Wangjiazhuang is similar to that of most loess profiles (Figure 6). The Wangjiazhuang ground fissure, f1, is dominated by horizontal pulling and cracking in the shallow surface part, which shows a near-vertical state, with a large degree of near-surface tension, and the depth of the cracking is related to the depth of the tectonic joints. Ground fissure f2 is located at the edge of the funnel, with a large degree of openness at the surface, showing a funnel-like shape in the profile, with a depth of nearly 1 m. The depth of its development is related to the amount of collapsible settlement.

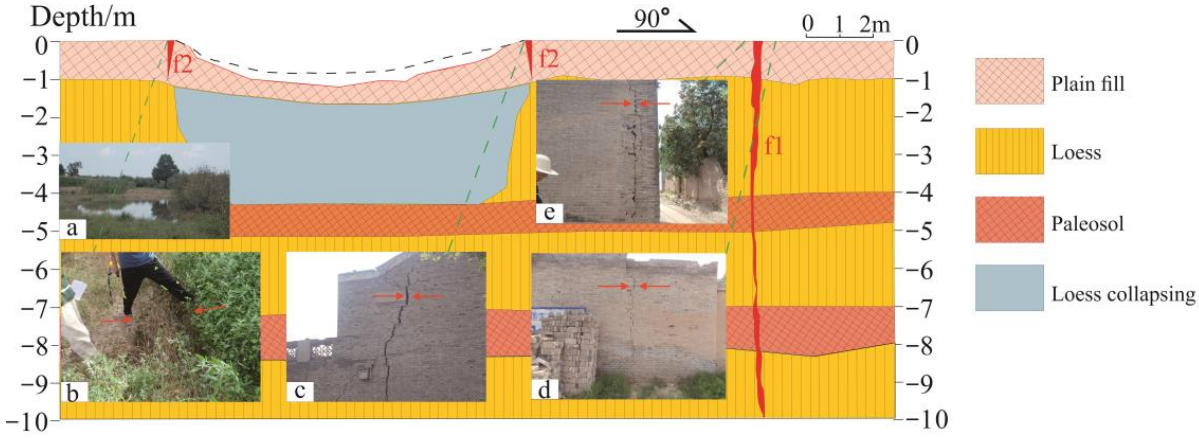

Figure 6. Fissure profile structure: (**a**) pool full view; (**b**) fissure on west side of pool; (**c**) fissure on east side of pool; (**d**) fissure on east side of joint; (**e**) fissure on west side of joint.

3.3. Destruction Characteristics

The Wangjiazhuang ground fissure runs through houses, roads, and farmland, causing great damage. S1–S11 show some typical damage points. Ground fissure f1 passes through and along its line of houses subjected to tensile stresses; the houses show varying degrees of damage, the cracks have degrees of tension of about 0.1 cm to 7 cm, and the morphology is mostly nearly vertical. The most severely damaged of these houses were demolished, with cracks up to 7 cm wide (S9). In addition, the damage caused by ground fissure f2 showed circular damage, resulting in severe cracks in the surrounding houses and large-scale sinkholes on the farmland, with the cracks in the houses showing near-vertical cracking and crack openings ranging from 1 to 5 cm; the maximum width of the sinkholes was 80 cm, and the maximum depth was 1.1 m (Figure 7).

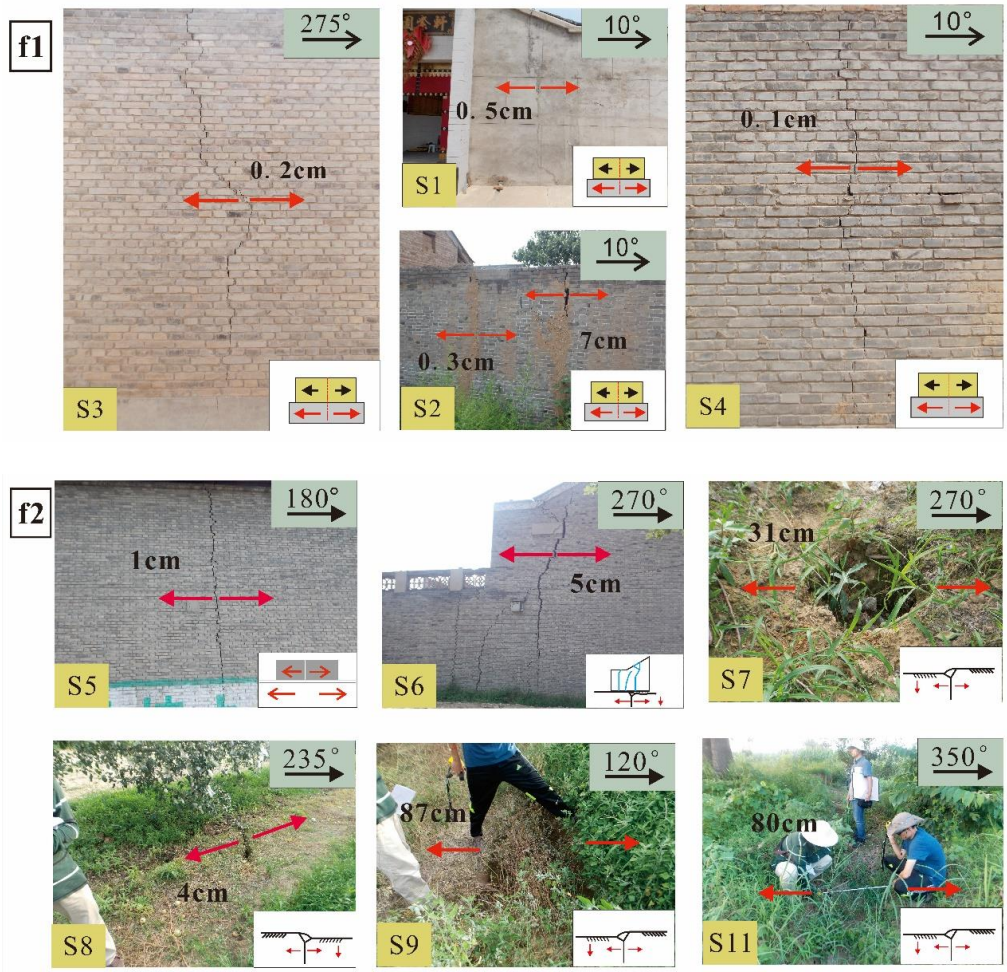

Figure 7. Characteristics of the damage and typical photos. The arrows and angles in the top right corner represent mirrors.

4. Discussion

In the Emei Platform of the Yuncheng Basin, two fissures in Wangjiacun exhibit distinct morphological characteristics and patterns of destruction, suggesting significant differences in their genesis mechanisms. Among them, fissure f1 is closely related to regional tectonic joints in the loess tableland area, while fissure f2 and fissure f2-1 are closely associated with differential loess collapse resulting from surface water infiltration.

4.1. Regional Tectonic Dynamics

The geographic location of the Fenwei Basin is very special; due to the uplift of the Tibetan Plateau, the eastward extrusion of the Gan-Qingdao Massif, the levitation of the Ordos Massif, and the incongruity of the South China–North China Plate and other regional dynamics, the Fenwei Basin is in a tension stress environment, and the Fenwei Basin ground fissures were formed under the action of this same tectonic stress [5]. Yuncheng Basin is one of the sub-basins of Fenwei Basin, and its stress field is dominated by the horizontal tensile action in the north-west direction, with the main compressive stress orientation of 30~60°and the asserted stress orientation of 280~340°. The strike of ground fissures in the Yuncheng Basin is dominated by the NE direction, which is consistent with the direction of the main compressive stress in the basin and is closely related to the tensile stress field in the NW direction in the basin. Under this stress field, the Yuncheng Basin is prone to tensile ground fissures parallel to the main compressive stress.

The tectonic strain field in the Shanxi graben is dominated by NW-SE tensile tension, which is manifested as a dextral strike-slip zone [5]. The study area is located on top of the

Emei Plateau in the Yuncheng Basin of Shanxi Province, and the faults surrounding the study area are right-handed strike-slip in nature. These fractures with right-handed natures create tensile stresses in the NW direction (Figure 8). The study area is dotted with loess, which has very low tensile strength and ultimate tensile strain, and hence, NE-oriented tectonic joints are developed in the area. In contrast, the direction of ground fissure f1 in the study area is NNE-SSW orientated, which is approximately the same as the direction of the tectonic joints. The formation of ground fissure f1 is closely related to NE-trending tectonic joints and is the tectonic basis of regional ground fissures. Ground fissure f1 in the study area was formed on the original loess joints at the rupture, and ground fissure f1 is directly controlled by the loess tectonic joints.

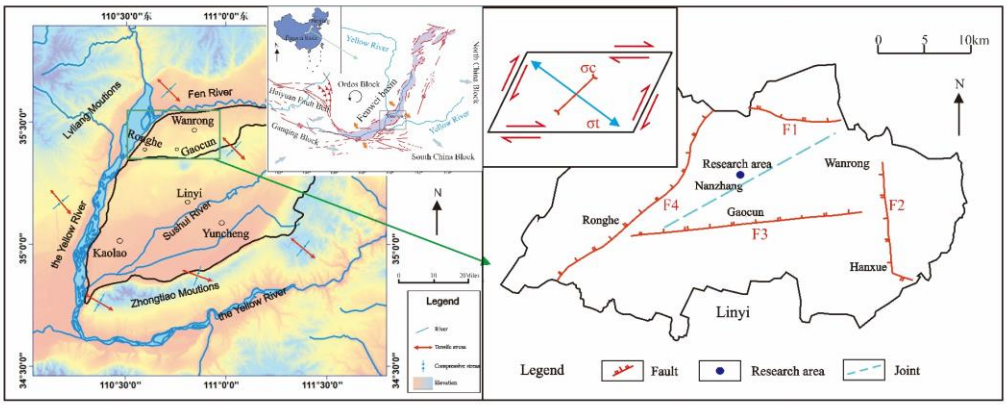

Figure 8. Tectonic stress-driven fissure formation; F1—northern edge of the Emei Plateau Fault, F2—Xishe-Zaidian Fault, F3—Wusu-Jiacun Fault, F4—eastern part of the Yellow River Valley Fault.

4.2. Structure and Properties of Loess

The structural characteristics of loess facilitate surface water infiltration, while the alternation of loess and ancient soils leads to the aggregation of water flow. Due to its collapsibility when encountering water, loess undergoes differential settlement, forming ground fissures.

The structural properties of soil are expressed as the ability to maintain the original structural state without being destroyed, including the shape and size of the particles and the size of the pores of the soil body. Loess is one of the main materials studied in terms of soil structural properties [34,35]. Loess has a large pore structure due to the environment in which it is formed, with large particles, point contacts between particles, and large pores, a structure that makes it very easy for water to enter the soil. Most of the stratigraphy in the loess region exists in a loess–paleosol cyclic manner; however, there are permeability differences between loess and paleosol. Loess layers typically have higher porosity, better permeability, and greater water-storage capacity, making them prone to forming aquifers, while ancient soils tend to form aquicludes. Because of these permeability differences, water flow tends to collect in the loess layer above the ancient soil layer after entering the soil mass.

The impermeability of the ancient soil layer causes water flow to collect in the loess layer. Upon encountering water, loess undergoes settlement due to its collapsibility. The collapsibility of loess refers to its property of significant additional settlement when the soil structure is rapidly disrupted under certain pressure conditions after being soaked with water. The unique collapsibility of loess poses significant safety hazards, closely related to the formation of ground fissures. Simultaneously, two-year InSAR data processing was conducted in the study area from 2017 to 2019, revealing significant subsidence in depressions where water is stored. The InSAR results indicate that the maximum settlement in this area is 1 cm and the maximum rate of settlement is 0.5 cm. The soil in the vicinity of circular ground fissure f2 in the study area consists of collapsible loess. Due to the topographical influence, the depressions with water storage conditions have advantages in collecting water, gathering a large amount of water sources in the area. Therefore, the

subsidence due to collapsibility of loess in this area is greater than that in surrounding areas, resulting in uneven differential settlement on the surface, generating tensile stress in the soil and leading to cracking, ultimately forming circular ground fissure f2 around the depressions where water is stored (Figure 9).

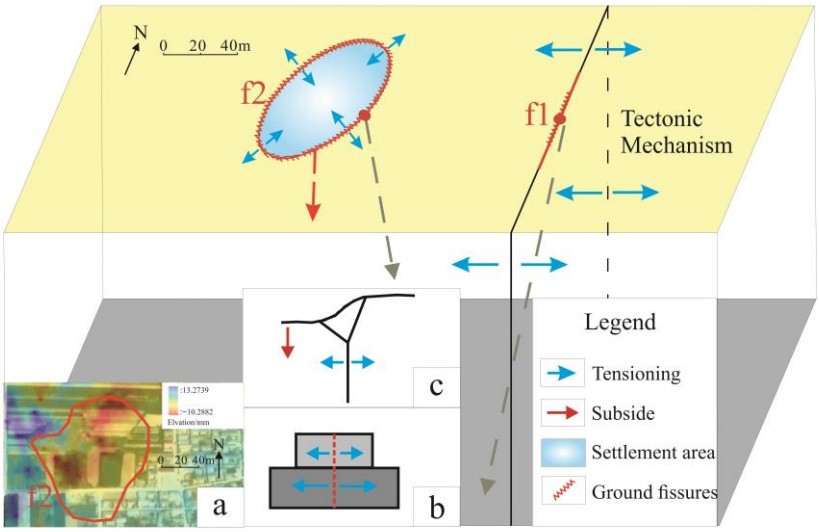

Figure 9. Differential settlement-induced ground fissure outcrops: (**a**) InSAR data-processing charts; (**b**) F1 mode chart; (**c**) F2 mode chart.

4.3. Impact of Surface Water

Surface water converging in the pool contributed to the collapse deformation of the loess at the shallow surface, and the tensile stresses generated by gravity bending contributed to the cracking of the shallow surface soil to form ground fissures.

When the infiltrating water body infiltrates to the top of the palaeosol, the water migration is mainly horizontal; the continuous accumulation of water at the top of the palaeosol results in upward water transport, and the shape of the infiltration shows a normal triangular shape (Figure 10).

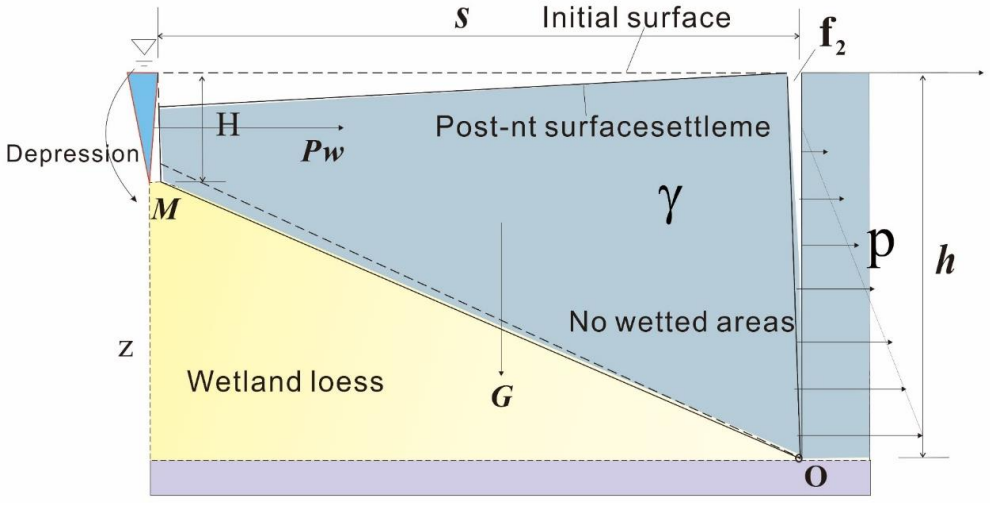

Figure 10. Ground fissure f2 gravity-bending mechanism of seam formation; G—gravity of collapsed soil mass, H—depth of tectonic joints, h—depth of burial of ancient soil, S—distance between the ground fissure and the center of the pool, γ—the bulk weight of the soil, pw—total water pressure.

In order to better quantify the mechanism of gravity bending of the collapsible loess ground fissure, f2, into a fissure, the following assumptions are made: (1) Only the bottom point seepage is considered in the impoundment depressions, and side seepage is

ignored; (2) collapsed loess and non-collapsed loess are completely disconnected, with no mechanical or hydraulic connection; (3) the loess is a homogeneous soil body with a uniform distribution of densities; (4) all loess within the wetting front undergoes collapse, and it occurs in a straight line.

Therefore, when the depth of burial of the paleo-soil is known, there exists a maximum critical value of SC for the cantilever beam such that the soil body just reaches moment equilibrium.

From the figure, it can be assumed that the process of crack formation is approximated as a folding of a cantilever beam, with the axis of rotation at point O (Figure 8), and the gravity of the isolating soil mass is as follows:

$$G = \frac{\gamma S_c (H + h)}{2} \tag{1}$$

where G is the gravity of collapsed soil mass, H is the depth of tectonic joints, h is the depth of the burial of ancient soil, S_c is the distance between the ground fissure and the center of the pool, and γ is the bulk weight of the soil.

The total water pressure in the pool is as follows:

$$P_w = \frac{1}{2}\gamma_w H^2 \tag{2}$$

where P_w is the total water pressure; γ_w is the bulk weight of water.

Assuming that the depth of fissure opening is straight through the top of the ancient soil and is approximately vertical, the following is based on the active soil pressure:

$$K_a = \tan^2\left(45^\circ - \frac{\varphi}{2}\right) \tag{3}$$

$$E_a = \frac{1}{2}\gamma h^2 K_a - 2ch\sqrt{K_a} + \frac{2c^2}{\gamma} \tag{4}$$

where K_a is the Rankine active earth pressure coefficient, E_a is Rankine active earth pressure, c is soil cohesion, and φ is the soil internal friction angle.

Based on the moment equilibrium, the following can be obtained:

$$G \cdot \left(\frac{1}{3} S_c \frac{2H + h}{H + h}\right) = \frac{1}{3} E_a \left(h - \frac{2c}{\gamma\sqrt{K_a}}\right) + P_w \left(h - \frac{2H}{3}\right) \tag{5}$$

By joining the above two equations, the critical cracking distance can be found as follows:

$$S_c = \sqrt{\frac{\left[\left(\gamma h^2 \tan^2\left(45^\circ - \frac{\varphi}{2}\right) - 4ch\tan\left(45^\circ - \frac{\varphi}{2}\right) + \frac{4c^2}{\gamma}\right)\left(h - \frac{2c}{\gamma\tan\left(45^\circ - \frac{\varphi}{2}\right)}\right) + \gamma_w H^2 (3h - 2H)\right]}{\gamma(2H + h)}} \tag{6}$$

From the above equation, it can be seen that the cracking of loess cracks caused by seepage is closely related to the depth of tectonic joints in addition to the cohesive force of the soil, the friction angle of the soil, the soil's bulk weight, and the depth of the paleosol, as well as the depth of the tectonic joints.

5. Conclusions

In this paper, the development characteristics and formation mechanism of ground fissures in Wangjiacun were studied through a detailed field geological survey of ground fissures, and the following conclusions were drawn:

(1) Three ground fissures were developed in Wangjiacun. Fissure f1 was linearly distributed, with a length of 334 m, which caused houses to show horizontal tension cracks; fissure f2 was a circular fissure, with a length of 720 m, and the fissure appeared to be

circularly cracked around the pool; at the same time, linear fissure f2-1 existed on the edge of the pool, with a length of 110 m.

(2) The combined effect of the regional stress field and faults led to the emergence of a north-east-oriented tectonic joint in the study area, which created north-west-south-east-oriented tensile stress, prompting the formation of ground fissure f1.

(3) The pool on the west side of the study area prompted surface water to pool in the area due to natural topographic conditions, and differential settlement was caused by water encountered by the collapsible loess, and the tensile stress generated by gravitational bending during the settlement process prompted the formation of ground fissures f2 and f2-1. For the collapsible loess ground fissures, areas of concentrated drainage in densely built-up areas are susceptible to ground fissures.

(4) This study provides a theoretical basis for disaster prevention and the mitigation of ground fissures in loess areas and enriches the theory of ground fissure genesis. Future research could qualitatively discuss the relationship between loess characteristics and ground fissure formation.

Author Contributions: Conceptualization, F.L. and F.W. (Feiyong Wang); methodology, F.L.; software, F.L.; formal analysis, F.L.; investigation, F.L., F.W. (Fujiang Wang), G.L. and F.W. (Feiyong Wang); resources, F.L.; data curation, F.L.; writing—original draft preparation, F.L.; writing—review and editing, F.W. (Feiyong Wang); visualization, F.L.; project administration, F.W. (Feiyong Wang); funding acquisition, F.W. (Feiyong Wang). All authors have read and agreed to the published version of the manuscript.

Funding: This research was funded by the National Science Foundation of China (NO. 2022XAGG0400, 42207202, 42293351), the Fundamental Research Funds for the Central Universities (NO. 2-9-2021-014), the Research Fund for the Development of Higher Education Disciplines (NO. 2023XK106), the Key Laboratory Open Fund (NO. EFGD2021-05-02, EFGD2023004).

Institutional Review Board Statement: Not applicable.

Informed Consent Statement: Informed consent was obtained from all subjects involved in the study.

Data Availability Statement: The data have all been shown in the text.

Conflicts of Interest: The authors declare no conflicts of interest.

References

1. Ayalew, L.; Yamagishi, H.; Reik, G. Ground cracks in Ethiopian Rift Valley: Facts and uncertainties. *Eng. Geol.* **2004**, *75*, 309–324. [CrossRef]
2. Carpenter, M.C. *Earth-Fissure Movements Associated with Fluctuations in Ground-Water Levels near the Picacho Mountains, South-Central Arizona, 1980–84*; Geological Survey (U.S.): Reston, VA, USA, 1993.
3. Muniram Budhu, M.A. Earth Fissure Formation from the Mechanics of Groundwater Pumping. *Int. J. Geomech.* **2011**, *11*, 1–11.
4. Zhou, Z.; Yao, X.; Ren, K.; Liu, H. Formation mechanism of ground fissure at Beijing Capital International Airport revealed by high-resolution InSAR and numerical modelling. *Eng. Geol.* **2022**, *306*, 106775.
5. Peng, J.; Sun, X.; Lu, Q.; Meng, L.; He, H.; Qiao, J.; Wang, F. Characteristics and mechanisms for origin of earth fissures in Fenwei basin, China. *Eng. Geol.* **2020**, *266*, 105445. [CrossRef]
6. Pacheco-Martínez, J.; Hernandez-Marín, M.; Burbey, T.J.; González-Cervantes, N.; Ortíz-Lozano, J.Á.; Zermeño-De-Leon, M.E.; Solís-Pinto, A. Land subsidence and ground failure associated to groundwater exploitation in the Aguascalientes Valley, México. *Eng. Geol.* **2013**, *164*, 172–186. [CrossRef]
7. Plummer, T.W.; Ferraro, J.V.; Louys, J.; Hertel, F.; Alemseged, Z.; Bobe, R.; Bishop, L.C. Bovid ecomorphology and hominin paleoenvironments of the Shungura Formation, lower Omo River Valley, Ethiopia. *J. Hum. Evol.* **2015**, *88*, 108–126. [CrossRef] [PubMed]
8. Xue, L.; Gani, N.D.; Abdelsalam, M.G. Drainage incision, tectonic uplift, magmatic activity, and paleo-environmental changes in the Kenya Rift, East African Rift System: A morpho-tectonic analysis. *Geomorphology* **2019**, *345*, 106839. [CrossRef]
9. Lu, Z.; Zhang, Q.; Zhao, C.; Peng, J.; Ji, L. Deformation at longyao ground fissure and its surroundings, north China plain, revealed by ALOS PALSAR PS-InSAR. *Int. J. Appl. Earth Obs. Geoinf.* **2018**, *67*, 1–9. [CrossRef]
10. Yan, Y.; Huang, Q.; Xie, Y.; Liu, T.; Xu, Q.; Fan, F.; Wang, Y. Failure analysis of urban open-cut utility tunnel under ground fissures environment in Xi'an, China. *Eng. Fail. Anal.* **2021**, *127*, 105529. [CrossRef]
11. Holzer, T.L.; Davis, S.N.; Lofgren, B.E. Faulting Caused by Ground Water Extraction in Southcentral Arizona. *J. Geophys. Res.* **1979**, *84*, 603–612. [CrossRef]

12. Sarkar, I. The role of the 1999 Chamoli earthquake in the formation of ground cracks. *J. Asian Earth Sci.* **2004**, *22*, 529–538. [CrossRef]
13. Harris, R.C. A New Earth Fissure near Wintersburg, Maricopa County, Arizona; Arizona Geological Survey Open File Report; OFR-01-10; 2001; 22p. Available online: https://repository.arizona.edu/handle/10150/629630 (accessed on 16 March 2024).
14. Huizar-Álvarez, R.; Mitre-Salazar, L.M.; Marín-Córdova, S.; Trujillo-Candelaria, J.; Martínez-Reyes, J. Subsidence in Celaya, Guanajuato, Central Mexico implications for groundwater extraction and the neotectonic regime. *Geofísica Int.* **2011**, *50*, 255–270. [CrossRef]
15. Ye, S.; Carreón-Freyre, D.; Teatini, P.; Galloway, D. IGCP 641 Project: Mechanisms, Monitoring and Modeling Earth Fissure Generation and Fault Activation due to Subsurface Fluid Exploitation. *Acta Geol. Sin.—Engl. Ed.* **2019**, *93*, 165–168. [CrossRef]
16. Geng Dayu, L.Z. Ground fissure hazards in USA and China. *Acta Seismol. Sin.* **2000**, *13*, 466–476. [CrossRef]
17. Yang, C.-S.; Zhang, Q.; Zhao, C.-Y.; Wang, Q.-L.; Ji, L.-Y. Monitoring land subsidence and fault deformation using the small baseline subset InSAR technique: A case study in the Datong Basin, China. *J. Geodyn.* **2014**, *75*, 34–40. [CrossRef]
18. Qiao, J.; Peng, J.; Deng, Y.; Leng, Y.; Meng, Z. Earth fissures in Qinglong Graben in Yuncheng Basin, China. *J. Earth Syst. Sci.* **2018**, *127*, 10. [CrossRef]
19. Peng, J.-B.; Huang, Q.-B.; Hu, Z.-P.; Wang, M.-X.; Li, T.; Men, Y.-M.; Fan, W. A proposed solution to the ground fissure encountered in urban metro construction in Xi'an, China. *Tunn. Undergr. Space Technol.* **2017**, *61*, 12–25. [CrossRef]
20. Lu, Q.; Liu, Y.; Peng, J.; Li, L.; Fan, W.; Liu, N.; Sun, K.; Liu, R. Immersion test of loess in ground fissures in Shuanghuaishu, Shaanxi Province, China. *Bull. Eng. Geol. Environ.* **2020**, *79*, 2299–2312. [CrossRef]
21. Yang, C.; Lu, Z.; Zhang, Q.; Liu, R.; Ji, L.; Zhao, C. Ground deformation and fissure activity in Datong basin, China 2007–2010 revealed by multi-track InSAR. *Geomat. Nat. Hazards Risk* **2019**, *10*, 465–482. [CrossRef]
22. Liu, X.; Su, S.; Ma, J.; Yang, W. Deformation Activity Analysis of a Ground Fissure Based on Instantaneous Total Energy. *Sensors* **2019**, *19*, 2607. [CrossRef]
23. Chang, J.; Deng, Y.; Xuan, Y.; Yan, Z.; Wu, W.; He, J. The dynamic response of sites with earth fissures as revealed by microtremor analysis—A case study in the Linfen Basin, China. *Soil Dyn. Earthq. Eng.* **2020**, *132*, 106076. [CrossRef]
24. Peng, J.; Meng, L.; Lu, Q.; Deng, Y.; Meng, Z. Development characteristics and mechanisms of the Taigu–Qixian earth fissure group in the Taiyuan basin, China. *Environ. Earth Sci.* **2018**, *77*, 407. [CrossRef]
25. Zhang, F.; Yang, C.S.; Zhao, C.Y.; Liu, R.C. Monitoring of the Ground Fissure Activity within Yuncheng Basin by Time Series Insar. *ISPRS—Int. Arch. Photogramm. Remote Sens. Spat. Inf. Sci.* **2018**, *42*, 2251–2255. [CrossRef]
26. Sun, P.; Peng, J.-B.; Chen, L.-W.; Yin, Y.-P.; Wu, S.-R. Weak tensile characteristics of loess in China—An important reason for ground fissures. *Eng. Geol.* **2009**, *108*, 153–159. [CrossRef]
27. Li, Y.; Yang, J.; Hu, X. Origin of ground fissures in the Shanxi Graben System, Northern China. *Eng. Geol.* **2000**, *55*, 267–275. [CrossRef]
28. Wan, J.; Li, B.; Tan, C.; Feng, C.; Zhang, P. Formation mechanism of pumping-induced earth fissures associated with a pre-existing normal fault, Beijing, China. *Eng. Geol.* **2019**, *294*, 106361. [CrossRef]
29. Liu, N.; Feng, X.; Huang, Q.; Fan, W.; Peng, J.; Lu, Q.; Liu, W. Dynamic characteristics of a ground fissure site. *Eng. Geol.* **2019**, *248*, 220–229. [CrossRef]
30. Peng, J.-B.; Chen, L.-W.; Huang, Q.-B.; Men, Y.-M.; Fan, W.; Yan, J.-K. Physical simulation of ground fissures triggered by underground fault activity. *Eng. Geol.* **2013**, *155*, 19–30. [CrossRef]
31. Jia, Z.; Lu, Q.; Peng, J.; Qiao, J.; Wang, F.; Wang, S.; Zhao, J. Analysis and comparison of two types of ground fissures in Dali County in the Weihe Basin, China. *Environ. Earth Sci.* **2019**, *79*, 38. [CrossRef]
32. Zhu, J.; Qiao, J.; Wang, F.; Lu, Q.; Xia, Y.; Chen, R.; Zhao, H.; Dong, J. Development characteristics and formation analysis of the Liangjia Village earth fissure in the Weihe Basin, China. *Front. Earth Sci.* **2020**, *14*, 758–769. [CrossRef]
33. Lu, Q.; Qiao, J.; Peng, J.; Liu, Z.; Liu, C.; Tian, L.; Zhao, J. A typical Earth fissure resulting from loess collapse on the loess plateau in the Weihe Basin, China. *Eng. Geol.* **2019**, *259*, 105189. [CrossRef]
34. Hou, X.; Qi, S.; Liu, F. Soil Water Retention and Pore Characteristics of Intact Loess Buried at Different Depths. *Sustainability* **2023**, *15*, 14890. [CrossRef]
35. Niu, L.; Niu, H.; Zhao, Y.; Ge, L.; Guo, M.; Ren, W.; Wang, Y.; Zhang, A. Study on the Unified Mechanical Properties of Ili Undisturbed Loess under the Influence of Soluble Salt. *Sustainability* **2023**, *15*, 14717. [CrossRef]

Disclaimer/Publisher's Note: The statements, opinions and data contained in all publications are solely those of the individual author(s) and contributor(s) and not of MDPI and/or the editor(s). MDPI and/or the editor(s) disclaim responsibility for any injury to people or property resulting from any ideas, methods, instructions or products referred to in the content.